

Light-emitting properties of a strain-tuned microtube containing coupled quantum wells

H. L. Zhen (甄红楼), G. S. Huang (黄高山), S. Kiravittaya, S. L. Li (李世龙), Ch. Deneke, Dominic J. Thurner, Y. F. Mei (梅永丰), O. G. Schmidt, and W. Lu (陆卫)

Citation: *Appl. Phys. Lett.* **102**, 041109 (2013); doi: 10.1063/1.4789534

View online: <https://doi.org/10.1063/1.4789534>

View Table of Contents: <http://aip.scitation.org/toc/apl/102/4>

Published by the [American Institute of Physics](#)

Articles you may be interested in

[Strain states in a quantum well embedded into a rolled-up microtube: X-ray and photoluminescence studies](#)
Applied Physics Letters **96**, 143101 (2010); 10.1063/1.3373592

[Uniaxial and tensile strained germanium nanomembranes in rolled-up geometry by polarized Raman scattering spectroscopy](#)
AIP Advances **5**, 037115 (2015); 10.1063/1.4914916

[Vertically aligned rolled-up SiO₂ optical microcavities in add-drop configuration](#)
Applied Physics Letters **102**, 251119 (2013); 10.1063/1.4812661

[Optical properties of rolled-up tubular microcavities from shaped nanomembranes](#)
Applied Physics Letters **94**, 141901 (2009); 10.1063/1.3111813

[SiO_x/Si radial superlattices and microtube optical ring resonators](#)
Applied Physics Letters **90**, 091905 (2007); 10.1063/1.2472546

[System investigation of a rolled-up metamaterial optical hyperlens structure](#)
Applied Physics Letters **95**, 083104 (2009); 10.1063/1.3211115

Scilight

Sharp, quick summaries **illuminating**
the latest physics research

Sign up for **FREE!**



Light-emitting properties of a strain-tuned microtube containing coupled quantum wells

H. L. Zhen (甄红楼),^{1,2,a)} G. S. Huang (黄高山),^{3,a)} S. Kiravittaya,^{2,4} S. L. Li (李世龙),² Ch. Deneke,^{2,5} Dominic J. Thurmer,² Y. F. Mei (梅永丰),^{3,b)} O. G. Schmidt,^{2,6} and W. Lu (陆卫)^{1,b)}

¹State Key Laboratory of Infrared Physics, Shanghai Institute of Technical Physics, Chinese Academy of Sciences, Shanghai 200083, People's Republic of China

²Institute for Integrative Nanosciences, IFW Dresden, Helmholtzstr. 20, D-01069 Dresden, Germany

³Department of Materials Science, Fudan University, Shanghai 200433, People's Republic of China

⁴Department of Electrical and Computer Engineering, Faculty of Engineering, Naresuan University, Phitsanulok 65000, Thailand

⁵Laboratório Nacional de Nanotecnologia (LNNano), Rua Giuseppe Máximo Scolfaro 10000, Campinas, SP, CEP 13083-100, Brazil

⁶Material Systems for Nanoelectronics, Chemnitz University of Technology, Reichenhainer Str. 70, D-09107 Chemnitz, Germany

(Received 9 November 2012; accepted 11 January 2013; published online 29 January 2013)

Pre-stressed multi-layer nanomembranes are rolled-up into a microtube in order to tune the strain applied to the contained coupled GaAs quantum wells. Additional GaAs/AlAs adjusting layers were deposited on the top of the nanomembrane to alter the thickness/stiffness of the to-be-rolled nanomembrane. In this way, microtubes with an adjustable diameter and strain are possible from a single initial grown sample. The internal strain state in the microtube affects the energy levels of the quantum wells and their coupling, which can be probed sensitively by photoluminescence. We measure different strain relaxation in rolled-up nanomembranes which we explain using a gradual change of the longitudinal relaxation as the distance of the nanomembrane from the etching front varies. © 2013 American Institute of Physics. [<http://dx.doi.org/10.1063/1.4789534>]

Rolled-up nanotechnology, which employs bottom-up and top-down fabrication techniques via a strain-engineering route, has the ability to conveniently produce three-dimensional micro-/nano-structures by releasing arbitrarily shaped strained nanomembranes and thus has drawn ever-increasing attention.^{1–6} The fabricated structures typically possess a tube-like geometry^{1,2,7} and their applications in optics,^{8–14} mechanics,^{15,16} electronics,^{17–19} and even biology²⁰ have been explored. The physical properties of the nanomembranes were found to be significantly influenced by the intrinsic strain/stress,^{21–24} and thus can be tuned by the rolling process.^{25,26} Among all the physical properties, the optical properties of rolled-up microtubes have been studied most extensively since they can be easily probed by light emission measurements. For instance, the band structure of a quantum well (QW) embedded in the rolled up nanomembrane is significantly altered and the corresponding photoluminescence (PL) signals shift as the strain inside the nanomembrane varies along its thickness.^{26–29} Here, we explore in detail how the light emission from strained rolled-up nanomembranes with embedded coupled QWs can be controlled. Additional stiffening layers were used to change the position of the neutral strain plane and thus the profile of the strain can thus be changed intentionally in a continuous manner. The coupling between the two QWs was tuned effectively using strain, as is revealed in the PL spectra. Both uni- and bi-axial strain relaxations were detected in strained

nanomembranes with different thicknesses and curvatures. Herein, the bi-axial relaxation refers to relaxation in both longitudinal and tangential directions while the uni-axial relaxation indicates tangential relaxation. We found that the longitudinal strain gradually relaxes with increasing distance of the nanomembrane from the etching front because the unreleased part is mechanically constrained by the substrate. Our results improve the understanding of the strain state and its evolution in rolled-up nanomembranes.

The microtube structures are made from strained layers grown by solid source molecular beam epitaxy on GaAs (001) substrate. The sample structure is shown in Fig. 1(a). Starting from the substrate, first a buffer layer is grown to increase epitaxial quality, and then we grew a 20 nm AlAs sacrificial layer followed by the layer sequence, which rolled up during selective removal of the sacrificial layer in dilute HF (10%). The layer sequence consists of a 20 nm In_{0.2}Al_{0.2}GaAs strained layer, a 15 nm Al_{0.4}Ga_{0.6}As bottom barrier, a 4 nm GaAs QW (QW2), a 3 nm Al_{0.4}Ga_{0.6}As central barrier for coupling, a further 3 nm GaAs QW (QW1), and a 15 nm top barrier. Differing from previous work,^{1,25–30} five cycles of 30 nm GaAs/2 nm AlAs layers were deposited on top of this layer sequence as adjusting layers to change the total thickness and stiffness of the nanomembrane. The GaAs and AlAs in the stiffening layers can be selectively etched away by dilute citric acid/H₂O₂ mixture (the volume ratio of 50% citric acid to H₂O₂ is 4:1) and dilute HF acid (10%), respectively, and therefore, we can obtain microtubes with different diameters (caused by different nanomembrane thicknesses)^{1,31} from one initial sample by removing a different number of these additional stiff layers, thus providing a well-defined tuning parameter for the

^{a)}H. L. Zhen and G. S. Huang contributed equally to this work.

^{b)}Authors to whom correspondence should be addressed. Electronic addresses: yfm@fudan.edu.cn and luwei@mail.sitp.ac.cn.

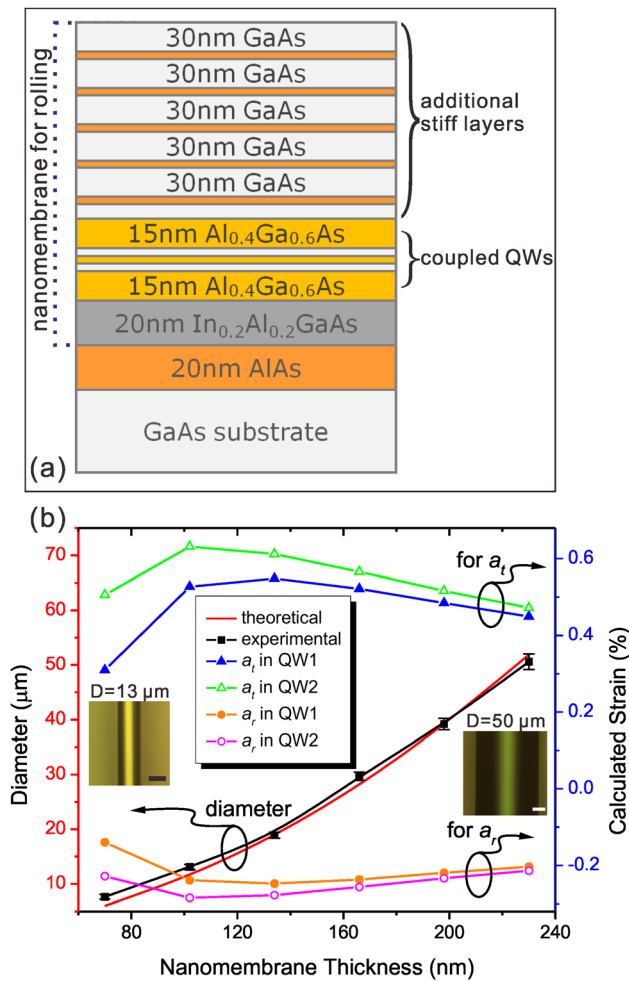


FIG. 1. (a) Layer sequence for the fabrication of rolled-up microtube containing coupled QWs in the walls. (b) Microtube diameter from optical microscopy as a function of the total thickness of the nanomembrane. The black squares and red line are experimental and theoretical results, respectively. The evolutions of calculated strains in both QWs are also plotted. a_t and a_r are lattice parameters along the tangential and radial directions, respectively. (For more details, please see main text.) The insets show typical optical images of microtubes with different diameters. Scale bar: 10 μm .

following systematic investigations. The morphological and geometrical properties were investigated using an optical microscopy (Zeiss AxioTech vario) connected to a camera (Zeiss AxioCam MR) for high-resolution images. Characterization of light emission was carried out at room temperature by using a HeCd laser operating at 442 nm as an excitation source. The laser was focused to a spot size of approximately 2 μm using a 50 \times microscope objective. The emitted light from the sample was collected by the same objective and the excitation source was removed by a long pass filter.

After the selective etching of the underneath AlAs layers, the strained nanomembranes were found to roll up into microtubes. The two insets in Fig. 1(b) show typical top-view optical images of microtubes with different diameters. The results prove that the strained layer (20 nm $\text{In}_{0.2}\text{Al}_{0.2}\text{GaAs}$) in the layer sequence can provide sufficient strain for the rolling process. Figure 1(b) shows the diameter of the microtube as a function of the total thickness of the nanomembrane. The black squares and corresponding error bars represent experimental results directly extracted from optical microscopy. One can see that for a nanomembrane

with five additional stiff layers, the microtube diameter is $\sim 50.6 \mu\text{m}$ while the nanomembrane without stiff layers yields microtubes with diameter of $\sim 7.6 \mu\text{m}$. This can be qualitatively explained as the removal of the additional stiff layer makes the nanomembrane “softer,” and the diameter will become smaller under the same initial strain. The experimental results suggest good controllability and reproducibility in geometry tuning by employing stiff layers. To elucidate this phenomenon quantitatively, diameters of the microtubes were calculated by adopting a macroscopic continuum mechanical model with a plain strain state (see solid line in Fig. 1(b)).^{32–34} Good agreement between experimental and theoretical results confirms the applicability of the model to the considered materials system. The application of additional stiff layers is also important for shifting the position of the neutral strain plane within the tube wall. For QW1 and QW2, the calculated strains based on changes in the lattice parameters along the tangential (a_t) and radial (a_r) directions³⁴ are plotted in Fig. 1(b). One can see different evolution tendencies in strains calculated from a_t and a_r , while the strains along the same direction in the two QWs are similar, indicating an excellent strain-tuning ability.

For the semiconductor QWs considered here, the electrons and heavy holes are localized in the confinement potentials in the conduction and valence bands, respectively. Although the two QWs are separated by a thin barrier layer (3 nm $\text{Al}_{0.4}\text{Ga}_{0.6}\text{As}$), the overlap between the wave functions of electrons/heavy holes could be large.^{35–37} For the sake of clarity, the ground state and the first excited state of electron are labeled as $e0$ and $e1$ while $hh0$ and $hh1$ for heavy hole case.³⁶ Therefore, four transition energies, $e0-hh0$, $e0-hh1$, $e1-hh0$, and $e1-hh1$, should exist in such coupled QWs, which is indeed proved both theoretically and experimentally in flat nanomembrane (upper plot in Fig. 2(a)). The lower plot in Fig. 2(a) shows the PL spectrum from the biggest microtube with a diameter of 50.6 μm , and four PL sub-bands can still be identified even before Gaussian deconvolution, although the peak positions redshift compared to those from the flat nanomembrane. The strain layer (20 nm $\text{In}_{0.2}\text{Al}_{0.2}\text{GaAs}$) is bi-axially compressed before releasing. When the nanomembrane is set free, the material in the strain layer tends to acquire its inherent lattice constant, making the nanomembrane bend upwards.¹ The strain applied to the QWs introduces an additional elastic energy into the system which modifies the band gap^{25–30} and hence also the four transition energies. The solution of the transition energies can be calculated theoretically by solving the Schrödinger equation with the elastic energy considered (Details can be found in Ref. 38). Figure 2(b) shows the band diagram and the calculated energy levels as well as wave functions of electron and heavy hole in the 50.6 μm microtube, where bi-axial strain relaxations are taken into account. The band diagram of the flat nanomembrane is also shown in dashed lines for comparison. The theoretical results explain the experimentally observed energy variation in Fig. 2(a).

With the removal of the additional stiff layers, the diameter decreases and the neutral strain plane³⁹ moves downwards due to the reduction in total nanomembrane thickness. This alters the strain status in the QWs which is reflected in the PL spectra. Figure 3(a) displays the PL spectra obtained

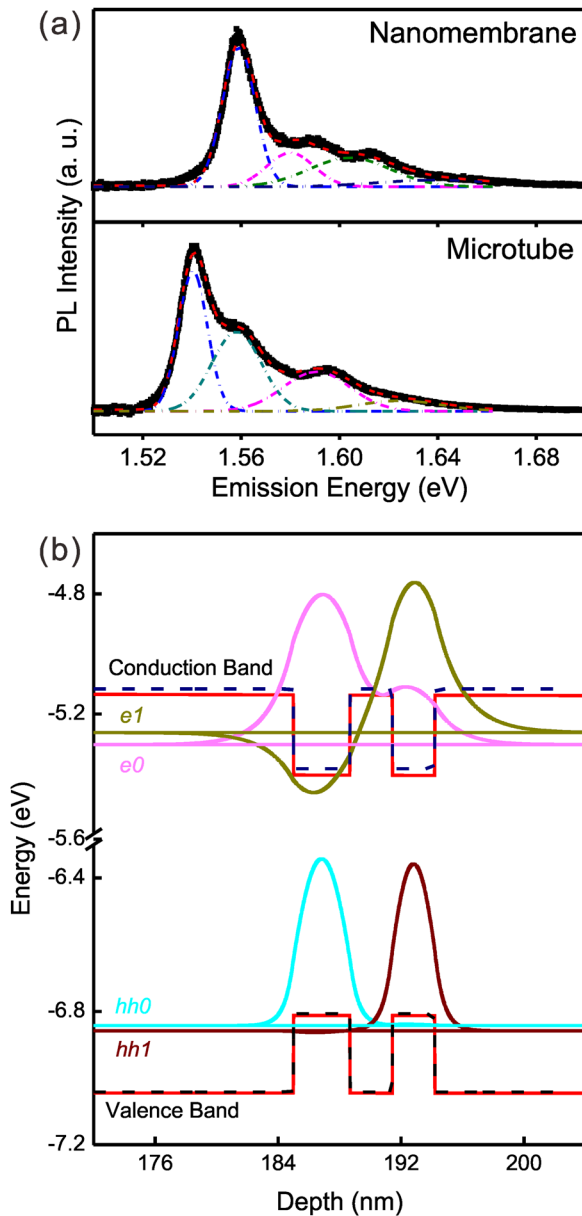


FIG. 2. (a) PL spectra from flat nanomembrane (upper) and microtube (lower). Both spectra can be fitted by four Gaussian peaks corresponding to optical transitions in coupled QWs. (b) Calculated band diagram of coupled QWs in microtube with a diameter of $50.6 \mu\text{m}$. The depth is calculated from the surface of the original nanomembrane. Energy levels and wave functions of electron and heavy hole are also plotted. The dashed lines show the band diagram of flat nanomembrane.

from microtubes with different diameters, and the shift of all the four sub-bands is easily identified. Here, we focus our discussion on the strongest PL band ($e0$ - $hh0$ transition). The calculated PL peak energy with bi-axial relaxation as a function of diameter is shown in Fig. 3(b) with red solid circles. The experimental results are well fitted when the number of residual stiff layers >2 . An obvious deviation is found when only one or two layers are left. In order to understand this phenomenon, the peak positions calculated from tangentially (i.e., uni-axially) relaxed nanomembranes are also given in Fig. 3(b) with blue open circles. We find out that the strain relaxation in large microtubes (i.e., thick nanomembrane) is bi-axial while in small microtubes (i.e., thin nanomembrane), the relaxation tends to be uni-axial. Normally the thin nano-

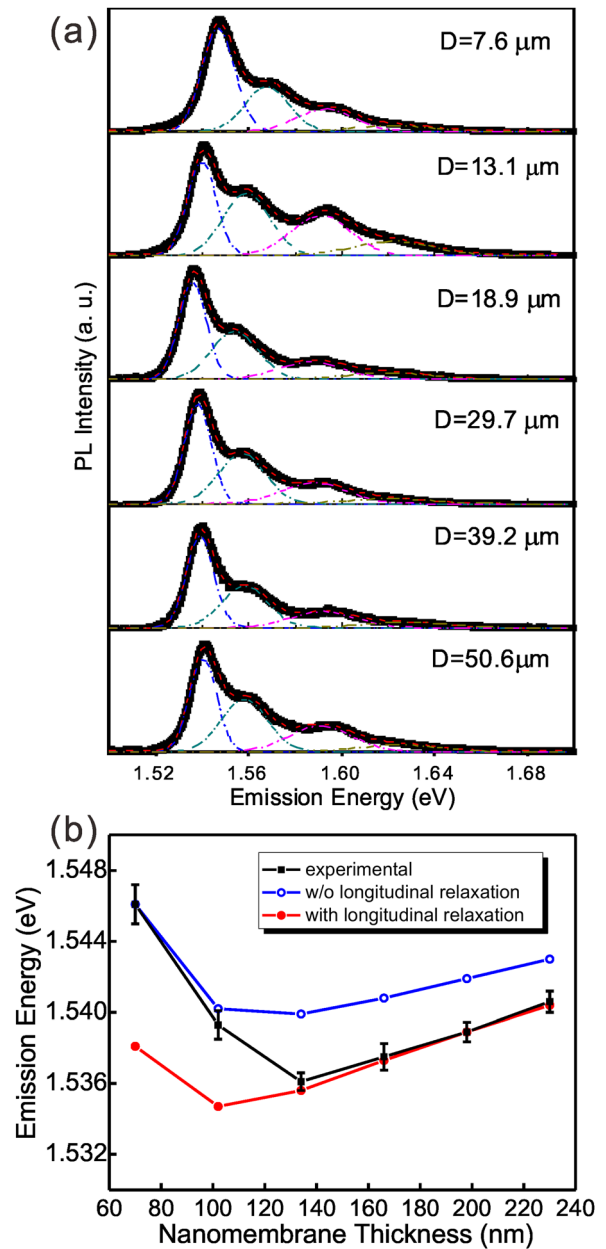


FIG. 3. (a) PL spectra from microtubes with different diameters. (b) Emission energy of the $e0$ - $hh0$ transition as a function of the microtube diameter. The black squares are experimental results. The blue open circles are calculated results when both longitudinal and tangential relaxations are considered. The red solid circles show the calculated results with only tangential relaxation.

membrane should easier relax, but the observed results can be reasonably explained if the measurement configuration is considered.

In our PL measurement setup, the signal is collected from the top, as shown in the sketch in Fig. 4(a). The nanomembrane distance between the measured spot and the etching front is half of the perimeter of the microtube's cross section (i.e., $\pi D/2$, where D is the diameter of the microtube), which varies for microtubes with different diameters. The longitudinal relaxation of the nanomembrane can be hindered by the unreleased part, which is still fixed to the substrate^{26,40} and would predominantly take place with increasing distance from the etching front.⁴⁰ Here, we suppose that the nanomembrane is completely relaxed in longitudinal direction after a

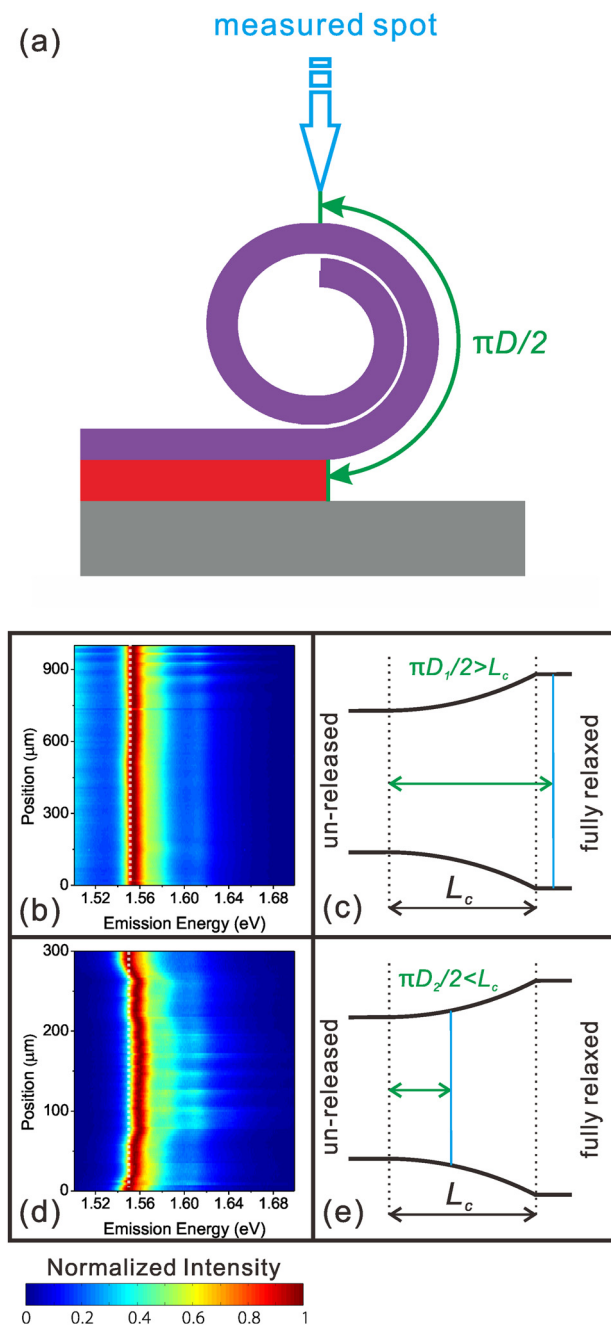


FIG. 4. (a) Diagram of the configuration for PL measurement. The distance between the measured spot and etching front is $\pi D/2$. (b) PL intensity map of a big microtube ($D_1 = 50.6 \mu\text{m}$) obtained by a line scan along the microtube. (c) Diagram illustrating that the measured spots in (b) are bi-axially relaxed. (d) PL intensity map of a small microtube ($D_2 = 7.6 \mu\text{m}$) obtained by a line scan along the microtube. (e) Diagram illustrating that the measured spots in (d) experience partial longitudinal relaxation.

critical underetching length L_c .⁴⁰ For microtubes with different diameters, the distance between the measured spot and the etching front is different, too, causing different relaxation states at the measured spots. We carried out PL measurements along the axes of two microtubes with different diameters, and the results are shown in Fig. 4. Figure 4(b) displays the results from the big microtube ($D_1 = 50.6 \mu\text{m}$). In this case, $\pi D_1/2$ is considered to be larger than L_c (Fig. 4(c)), and the nanomembrane undergoes complete bi-axial relaxation and thus the emission wavelength is constant along the whole microtube axis (Fig. 4(b)). For a small microtube with

$D_2 = 7.6 \mu\text{m}$, it is possible that $\pi D_2/2 < L_c$ (Fig. 4(e)), and the microtube is only partially relaxed along the axis except for the two ends. Therefore, in Fig. 4(d), one can see that the emission from the ends occurs at longer wavelengths.

In summary, we have fabricated microtubes with embedded coupled GaAs QWs by rolling pre-defined strained nanomembranes. The thickness of the nanomembrane, the diameter of the microtube, and even the strain state of the QWs can be well tuned by changing the number of additional GaAs/AlAs stiff layers, and the experimental results are explained by a continuum mechanical model. Both uni- and bi-axial strain relaxations exist as the longitudinal strain relaxation increases with distance from the etching front. The results presented here improve the understanding of the strain state in rolled-up structures and could be promising in future tube-based micro-/nano-optical-devices.

The authors thank Libo Ma, Stefan Harazim, and Daniel Grimm for technical support. This work is financially supported by the Natural Science Foundation of China (Nos. 51102049, 61008029, and 60906058), the CAS/SAFEA International Partnership Program for Creative Research Teams (09K4400DG0), Program for New Century Excellent Talents in University (No. NCET-10-0345), and Science and Technology Commission of Shanghai Municipality (Nos. 11PJ1400900, 12PJ1400500, and 12520706300). S. L. Li thanks the financial support from China Scholarship Council (CSC, File No. 2008617109).

¹V. Y. Prinz, V. A. Seleznev, A. K. Gutakovskiy, A. V. Chehovskiy, V. V. Preobrazhenskii, M. A. Putyato, and T. A. Gavrilova, *Physica E* **6**, 828 (2000).

²O. G. Schmidt and K. Eberl, *Nature* **410**, 168 (2001).

³G. S. Huang and Y. F. Mei, *Adv. Mater.* **24**, 2517 (2012).

⁴J. A. Rogers, M. G. Lagally, and R. G. Nuzzo, *Nature* **477**, 45 (2011).

⁵M. M. Roberts, L. J. Klein, D. E. Savage, K. A. Slinker, M. Friesen, G. Celler, M. A. Eriksson, and M. G. Lagally, *Nature Mater.* **5**, 388 (2006).

⁶J. A. Rogers, T. Someya, and Y. G. Huang, *Science* **327**, 1603 (2010).

⁷Y. F. Mei, G. S. Huang, A. A. Solovev, E. Bermúdez Ureña, I. Mönch, F. Ding, T. Reindl, R. K. Y. Fu, P. K. Chu, and O. G. Schmidt, *Adv. Mater.* **20**, 4085 (2008).

⁸T. Kipp, H. Welsch, Ch. Strelow, Ch. Heyn, and D. Heitmann, *Phys. Rev. Lett.* **96**, 077403 (2006).

⁹C. Strelow, H. Rehberg, C. M. Schultz, H. Welsch, C. Heyn, D. Heitmann, and T. Kipp, *Phys. Rev. Lett.* **101**, 127403 (2008).

¹⁰G. S. Huang, V. A. Bolaños Quiñones, F. Ding, S. Kiravittaya, Y. F. Mei, and O. G. Schmidt, *ACS Nano* **4**, 3123 (2010).

¹¹E. J. Smith, Z. W. Liu, Y. F. Mei, and O. G. Schmidt, *Nano Lett.* **10**, 1 (2010).

¹²T. R. Zhan, C. Xu, F. Y. Zhao, Z. Q. Xiong, X. H. Hu, G. S. Huang, Y. F. Mei, and J. Zi, *Appl. Phys. Lett.* **99**, 211104 (2011).

¹³S. Vicknesh, F. Li, and Z. T. Mi, *Appl. Phys. Lett.* **94**, 081101 (2009).

¹⁴F. Li and Z. T. Mi, *Opt. Express* **17**, 19933 (2009).

¹⁵Y. F. Mei, A. A. Solovev, S. Sanchez, and O. G. Schmidt, *Chem. Soc. Rev.* **40**, 2109 (2011).

¹⁶W. M. Li, G. S. Huang, J. Wang, Y. Yu, X. J. Wu, X. G. Cui, and Y. F. Mei, *Lab Chip* **12**, 2322 (2012).

¹⁷C. C. Bof Bufon, J. D. Arias Espinoza, D. J. Thurmer, M. Bauer, Ch. Deneke, U. Zschieschang, H. Klauk, and O. G. Schmidt, *Nano Lett.* **11**, 3727 (2011).

¹⁸D. J. Thurmer, C. C. Bof Bufon, Ch. Deneke, and O. G. Schmidt, *Nano Lett.* **10**, 3704 (2010).

¹⁹F. Cavallo, R. Somuang, and O. G. Schmidt, *Appl. Phys. Lett.* **93**, 143113 (2008).

²⁰G. S. Huang, Y. F. Mei, D. J. Thurmer, E. Coric, and O. G. Schmidt, *Lab Chip* **9**, 263 (2009).

²¹Y. F. Mei, S. Kiravittaya, S. Harazim, and O. G. Schmidt, *Materials Science & Engineering R: Reports* **70**, 209 (2010).

- ²²S. Kiravittaya, A. Rastelli, and O. G. Schmidt, *Appl. Phys. Lett.* **88**, 043112 (2006).
- ²³J.-H. Wong, B.-R. Wu, and M.-F. Lin, *J. Phys. Chem. C* **116**, 8271 (2012).
- ²⁴M. H. Huang, C. S. Ritz, B. Novakovic, D. C. Yu, Y. Zhang, F. Flack, D. E. Savage, P. G. Evans, I. Knezevic, F. Liu, and M. G. Lagally, *ACS Nano* **3**, 721 (2009).
- ²⁵S. Mendach, R. Songmuang, S. Kiravittaya, A. Rastelli, M. Benyoucef, and O. G. Schmidt, *Appl. Phys. Lett.* **88**, 111120 (2006).
- ²⁶Ch. Deneke, A. Malachias, S. Kiravittaya, M. Benyoucef, T. H. Metzger, and O. G. Schmidt, *Appl. Phys. Lett.* **96**, 143101 (2010).
- ²⁷K. Kubota, P. O. Vaccaro, N. Ohtani, Y. Hirose, M. Hosoda, and T. Aida, *Physica E* **13**, 313 (2002).
- ²⁸M. Hosoda, Y. Kishimoto, M. Sato, S. Nashima, K. Kubota, S. Saravanan, O. Vaccaro, T. Aida, and N. Ohtani, *Appl. Phys. Lett.* **83**, 1017 (2003).
- ²⁹N. Ohtani, K. Kishimoto, K. Kubota, S. Saravanan, Y. Sato, S. Nashima, P. Vaccaro, T. Aida, and M. Hosoda, *Physica E* **21**, 732 (2004).
- ³⁰D. J. Thurmer, Ch. Deneke, Y. F. Mei, and O. G. Schmidt, *Appl. Phys. Lett.* **89**, 223507 (2006).
- ³¹Ch. Deneke, C. Müller, N. Y. Jin-Phillipp, and O. G. Schmidt, *Semicond. Sci. Technol.* **17**, 1278 (2002).
- ³²M. Grundmann, *Appl. Phys. Lett.* **83**, 2444 (2003).
- ³³G. P. Nikishkov, *J. Appl. Phys.* **94**, 5333 (2003).
- ³⁴A. Malachias, Ch. Deneke, B. Krause, C. Mocuta, S. Kiravittaya, T. H. Metzger, and O. G. Schmidt, *Phys. Rev. B* **79**, 035301 (2009).
- ³⁵K. Sivalertporn, L. Mouchliadis, A. L. Ivanov, R. Philp, and E. A. Muljarov, *Phys. Rev. B* **85**, 045207 (2012).
- ³⁶G. Sun, Y. J. Ding, G. Y. Liu, G. S. Huang, H. P. Zhao, N. Tansu, and J. B. Khurgin, *Appl. Phys. Lett.* **97**, 021904 (2010).
- ³⁷Y. J. Chen, E. S. Koteles, B. S. Elman, and C. A. Armiento, *Phys. Rev. B* **36**, 4562 (1987).
- ³⁸P. Cendula, S. Kiravittaya, and O. G. Schmidt, *J. Appl. Phys.* **111**, 043105 (2012).
- ³⁹Y. F. Mei, S. Kiravittaya, M. Benyoucef, D. J. Thurmer, T. Zander, Ch. Deneke, F. Cavallo, A. Rastelli, and O. G. Schmidt, *Nano Lett.* **7**, 1676 (2007).
- ⁴⁰P. Cendula, S. Kiravittaya, Y. F. Mei, Ch. Deneke, and O. G. Schmidt, *Phys. Rev. B* **79**, 085429 (2009).